Scientific Research Publishing

Advances in Nanoparticles, 2018, 7, 1-10
http://www.scirp.org/journal/anp
ISSN Online: 2169-0529
ISSN Print: 2169-0510

Effect of Cu^{2+} Doping on Structural and Optical Properties of Synthetic $Zn_{0.5}Cu_xMg_{0.5-x}Fe_2O_4$ (x = 0.0, 0.1, 0.2, 0.3, 0.4) Nano-Ferrites

Badawi M. Ali[1], Mohamed A. Siddig[1,2], Yousef A. Alsabah[1,3], Abdelrahman A. Elbadawi[1,4*], Abdalrawf I. Ahmed[1]

[1]Department of Physics, Faculty of Science and Technology, Al Neelain University, Khartoum, Sudan
[2]Department of Physics, Faculty of Science, Albaha University, Al Baha, KSA
[3]Department of Physics, Faculty of Education and Applied Science, Hajjah University, Hajjah, Yemen
[4]Faculty of Basic Studies, Future University, Khartoum, Sudan
Email: *bahlaoy.ab@gmail.com

How to cite this paper: Ali, B.M., Siddig, M.A., Alsabah, Y.A., Elbadawi, A.A. and Ahmed, A.I. (2018) Effect of Cu^{2+} Doping on Structural and Optical Properties of Synthetic $Zn_{0.5}CuxMg_{0.5-x}Fe_2O_4$ (x = 0.0, 0.1, 0.2, 0.3, 0.4) Nano-Ferrites. *Advances in Nanoparticles*, **7**, 1-10.
https://doi.org/10.4236/anp.2018.71001

Received: November 29, 2017
Accepted: February 20, 2018
Published: February 23, 2018

Abstract

The samples of $Zn_{0.5}Cu_xMg_{0.5-x}Fe_2O_4$ nanoparticle ferrites, with x= 0.0, 0.1, 0.2, 0.3, 0.4 were successfully synthesised. Structural and optical properties were investigated by X-ray Diffraction (XRD), Fourier Transform Infrared spectroscopy (FTIR) and UV-visible spectroscopy. The structural studies showed that all the samples prepared through the Co-precipitation method was a single phase of a face-cantered-Cubic (FCC) spinel symmetry structures with space group (SG): Fd-3m. In the series $Zn_{0.5}Cu_xMg_{0.5-x}Fe_2O_4$, the lattice parameter was found to be 8.382 Å for x = 0 and was found to increase with copper concentration. The grain size obtained from the XRD data analyses was found to be in the range of 15.97 to 28.33 nm. The increased in the grain size may be due to the large ionic radius of Mg^{2+} (0.86 Å) compared with Cu^{2+} (0.73 Å). The FTIR spectroscopy confirmed the formation of spinel ferrite and showed the characteristics absorption bands around 580, 1112, 1382, 1682, 1632 and 2920 cm^{-1}. The energy band gap was calculated for samples were found to be in the range 4.04 to 4.67 eV.

Keywords

Ferrite, Nanostructure, Spinel Structure, X-Ray Diffraction XRD, FTIR, UV.vis

1. Introduction

Nanotechnology is considered one of the modern sciences that look for design-

ing the smallest apparatus and it concentrates basically on substituting the particle structures or the atomic parts of the material towards realizing new structures and with the economic cost which should not exceed the raw material [1] [2]. The Nanotechnology is also regarded as the basic future sciences that will gain an increasing demand in the field of industry, medicine and transferring and transport sector and also in the field of aviation, space and telecommunication [3] [4]. The biological, chemical and material properties in the Nano-size, differ from the basic shapes and properties of an atom or material itself [5] [6] [7]. Ferrites are chemical compounds with the formula of AB_2O_4, where A and B represent various metal cations, usually including iron [8] [9]. Ferrites are the well-known ferromagnetic materials that consist mainly of ferromagnetic oxides and therefore, are electrically insulating. Ferrites are widely used in high-frequency applications/because an alternating current (AC) field does not induce undesirable eddy currents in an insulating material [10] [11]. Properties of ferrites are dependent upon several factors such as composition, a method of preparation, substitution and doping of different captions, sintering temperature and time, sintered density, grain size and their distribution. Apart from the fact that they have very complex structures, their physical properties themselves are dependent on a number of valence electrons of the divalent or trivalent metal ions of tetrahedral (A) and octahedral (B) sites. Several attempts have been made to enhance the qualities of ferrites by employing various methods. The most general method is the incorporation of same suitable nonmagnetic/diamagnetic impurities at the A or B sites [12] [13] [14]. Many of synthesis methods were considered in previous studies for produce the Nano-particles with size in the range of 2 - 100 nm. Among these methods are co-precipitation, hydrothermal and sol-gel methods [7] [15] [16].

In this work, Nano-ferrite samples of $Zn_{0.5}Cu_xMg_{0.5-x}Fe_2O_4$ were synthesised using co-precipitation method. The structural and optical properties were studied using X-ray diffraction (XRD), Fourier Transform Infrared spectroscopy (FTIR) and UV-Visible spectroscopy. The main purpose is to study the effect of copper substituted magnesium in the $Zn_{0.5}Cu_xMg_{0.5-x}Fe_2O_4$ Nano-ferrites.

2. Material and Method

The samples $Zn_{0.5}Cu_xMg_{0.5-x}Fe_2O_4$ ferrites nano-crystalline powder with compositions (x = 0.0,0.1,0.2,0.3,0.4) were prepared using high purity (Sigma,98%) of zinc nitrate [$Zn(NO_3)_2{\cdot}6H_2O$(96%)], magnesium nitrate [$Mg(NO_3)_2$(99%)] copper nitrate [$Cu(NO_3)_2{\cdot}3H_2O$(99%)] Ferric nitrate [$Fe(NO_3)_2{\cdot}9H_2O$(98%)] and Sodium hydroxide 96% were used as primary components. A Specified amount of Oleic acid was added to the solution as surfactant and coating material. The solution of $Fe(NO_3)_3{\cdot}9H_2O$, 0.4 M (25 ml), $Mg(NO_3)_2{\cdot}6H_2O$, 0.2 M (25 ml), $Cu(NO_3)_2{\cdot}3H_2O$, and $Zn(NO_3)_2{\cdot}6H_2O$ were first mixed and then slowly added 3 molarities of NaOH. The PH of the solution was constantly monitored as the NaOH solution was added. The reactant was constantly stirred using magnetic

stirrer unit a pH level of (11-12) [7]. The liquid precipitate was then brought to a reaction temperature of 80˚C and stirred for one hour. At this stage, the product contains some associated water which was removed by heating at 450˚C for 6 hours in temperature controlled muffle furnace Vulcan A-550 at a heating rate 10˚C/min. The final product obtained materials were ground into powder and then made ready for characterization using various techniques.

X-ray diffraction (XRD) data collected by Shimadzu 6000 X-ray diffract meter with Cu-kα radiation of a wavelength of λ = 1.5406 Å. At room temperature, with a nickel filter operating at 40 KV, 40 mA the data collected for the 2θ in 0.02-step size and five-second count time in 20˚ - 80˚ range. The MDI jade 0.5 programs used for the XRD date analysis. The crystallite size (D) calculated by Scherer equation [17].

At room temperature, the transmittance mode investigated for the sample by a (Satellite FTIR 5000 of the wavelength range of 400 to 4000 cm^{-1}) where the important bands and peaks of spinel structure can be assigned. A Fourier transform infrared spectroscopy collected by KBr pellet method, the material mixed with KBr of ratio 1:100 for FTIR measurement between 400 and 2000 cm^{-1} [17] [18].

The UV-Visible absorption was investigated by UV Mini 1240 manufactured by Shimadzu company-Japan. Hydrochloric acid HCl was used as a reference for 100% absorbance [19].

3. Results and Discussion

3.1. X-Ray Result

Symmetry is important in the study of structural and optical properties of the nanoparticle ferrites. **Figure 1** shows crystalline phases determination of the crystal structure, the lattice parameters and the space group. The spinal of single phase $Zn_{0.5}Cu_{0.4}Mg_{0.1}Fe_2O_4$ nano-ferrite, with composition (x = 0.4) after analysing the XRD patterns are well indexed using MDI jade 5 and full proof. The crystal structure is found to be cubic with space group Fd3m.The fined peaks are indexed as the following (220), (311), (400), and (511). The crystallite size, the lattice constant, volume, space group and density are listed in **Table 1**, and the crystal size is calculated using Scherer's equation [17] [18].

$$D = \frac{0.94\lambda}{\beta \cos\theta} \tag{1}$$

where D is the average crystallite size, θ is the angle, λ is the incident of X-ray wavelength, while β is the (FWHM) of the highest intensity peak (311). The results of X-ray diffraction are listed in **Table 1**.

Figure 2 shows the intensity and 2θ for samples with a different concentration of copper crystalline size are found to the scattered in the range 20.94 nm up to 28.33 nm for different compositions. As the concentration of copper increases from x = 0.1 to 0.4, the lattice constant, *a*, increased from 8.375 Å to 8.397 Å. The increasing in lattice constant is attributed due to the larger ionic radius of

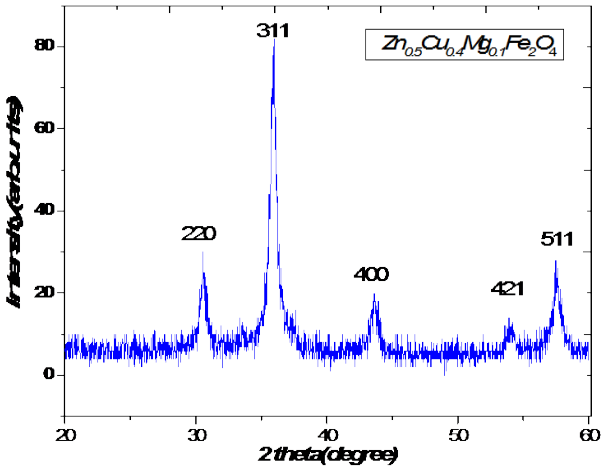

Figure 1. XRD patterns of $Zn_{0.5}Cu_{0.4}Mg_{0.1}Fe_2O_4$.

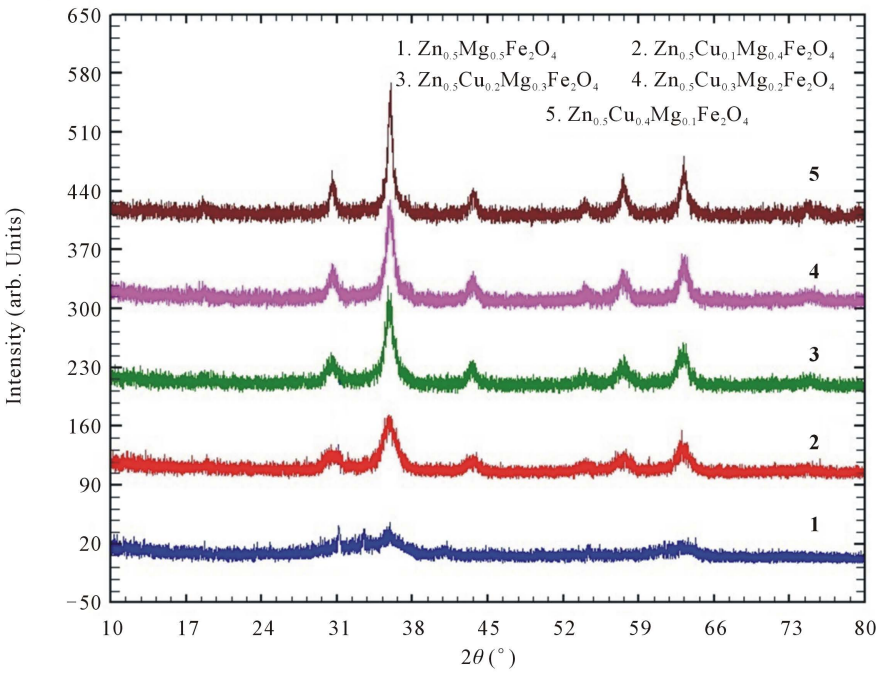

Figure 2. Comparison of (XRD) pattern for Cu-doped $ZnMgFe_2O_4$ spinel samples.

Table 1. Crystallite size (*D*), Lattice constant (*a*), volume (*v*) space group and density of $Zn_{0.5}Cu_xMg_{0.5-x}Fe_2O_4$ nano-ferrites: where (X = 0.0, 0.1, 0.2, 0.3, 0.4).

No	Samples	Crystallite size (nm)	Lattice constant (Å)	Volume (nm^3)	Space groups	Density (g/cm^{-3})
1	$Zn_{0.5}mg_{0.5}Fe_2O_4$	15.97	8.382	588.90	Fd-3m(227)	0.656
2	$Zn_{0.5}mg_{0.4}Cu_{0.1}Fe_2O_4$	23.96	8.375	587.4	Fd-3m(227)	0.634
3	$Zn_{0.5}mg_{0.3}Cu_{0.2}Fe_2O_4$	20.94	8.380	588.5	Fd-3m(227)	0.650
4	$Zn_{0.5}mg_{0.2}Cu_{0.3}Fe_2O_4$	20.94	8.381	588.7	Fd-3m(227)	0.655
5	$Zn_{0.5}mg_{0.1}Cu_{0.4}Fe_2O_4$	28.33	8.397	591.1	Fd-3m(227)	0.657

Mg^{2+} (0.86 Å) compared with Cu^{2+} (0.73 Å) [4]. The results showed that the lattice parameter, a, was increased with copper concentration and attributed to the smaller ionic radius of magnesium nanoferrite by co-precipitation. Yue *et al.* [20], worked on the effect of copper on electromagnetic properties of $(Mg_{0.5-x}Cu_x Zn_{0.5})O(Fe_2O_3)_{0.98}$ ferrite and found that the density, grain size, permeability, curie temperature increased. Rezlescu *et al.* [21] also reported that the sintered density and resistivity of $Mg_{0.5-x}Cu_xZn_{0.5} + 0.5MgOFe_2O_4$ ferrite increased up to X = 0.3 whereas, permeability increased up to X = 0.4 [14]. However, in this study; the effect of copper substituted magnesium Nano-ferrites by co-precipitation technique showed the lattice parameter increases from x = 0.1 to 0.4 when the Cu^{2+}concentration was increased.

From Table 1 we can observe that the density and volume increase with increasing Cu content. The increase in density and volume may be due to the ionic of constituent ions. After analysing the XRD data, the structural studies showed that all the samples prepared through the co-precipitation method are single phase of a face-centred Cubic (FCC) spinel and the symmetry structures with space group SG: Fd-3m.

Figure 3 shows the relation between lattice parameters and concentration of copper. It can be observed that the lattice constants are increased as the concentration of copper further increase.

3.2. FTIR Analysis

Functional groups of the synthesize $Zn_{0.5}Cu_xMg_{0.5-x}Fe_2O_4$are investigated by FTIR spectroscopy in the range of 400 to 4000 cm^{-1}. Figure 4 shows the spectra of all the ferrites has been used to locate the band positions which is listed in Table 2. In the present study the absorption bands v_1, v_2, v_3, v_4 and v_5 are found to be around 580, 1112, 1382, 1632 and 2920 cm^{-1}.

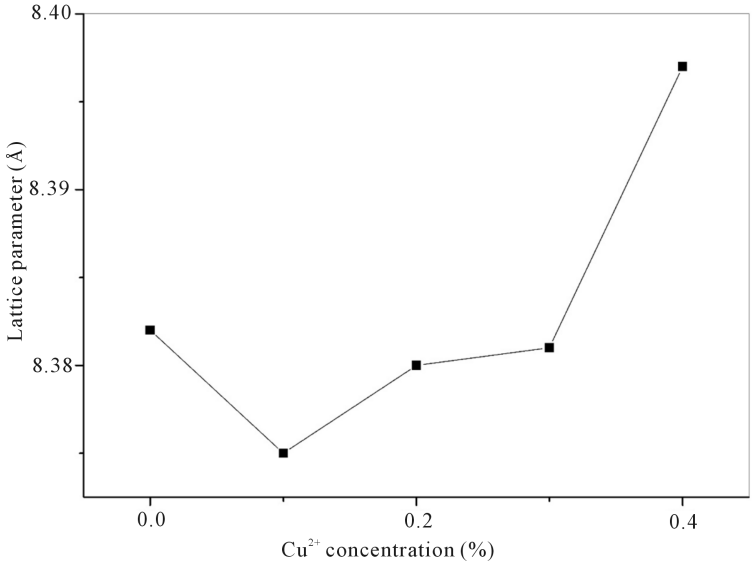

Figure 3. The relation between lattice parameters and concentration.

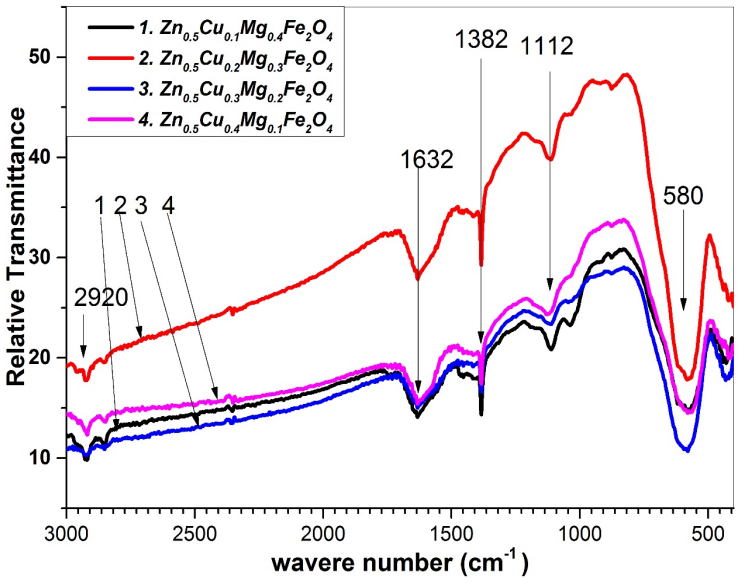

Figure 4. FTIR spectra of $Zn_{0.5}Cu_xMg_{0.5-x}Fe_2o_4$ Nano ferrites of different concentration of Cu.

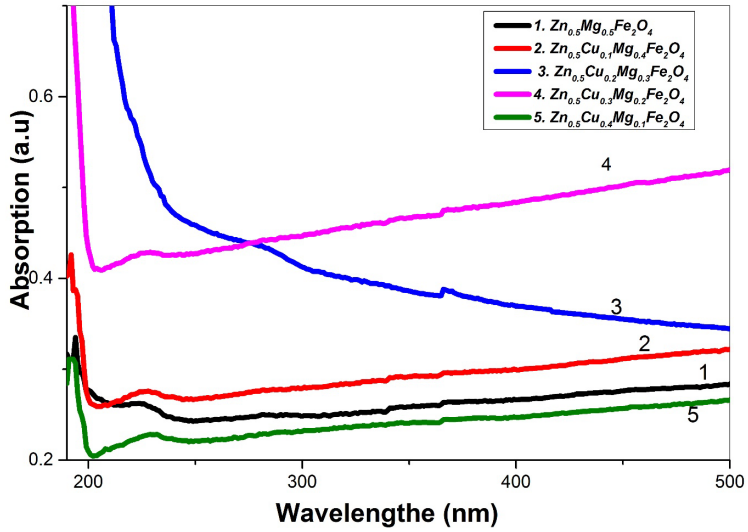

Figure 5. Diffused UV-visible spectra of $Zn_{0.5}Cu_xMg_{0.5-X}Fe_2O_4$ with varying Cu^{2+} dopant as (1) X = 0.0, (2) X = 0.1, (3) X = 0.2, (4) X = 0.3 and (5) X = 0.4 showing different band edge absorbance.

Table 2. Wave numbers and band gap energy of the $Zn_{0.5}Cu_xMg_{0.5-x}Fe_2O_4$ nano-ferrites samples.

Nano composites	ν_1	ν_2	ν_3	ν_4	ν_5	E_g (eV)
$Zn_{0.5}mg_{0.5}Fe_2O_4$	576	1112	1386	1637	2926	4.67
$Zn_{0.5}mg_{0.4}Cu_{0.1}Fe_2O_4$	576	1114	1387	1633	2923	4.63
$Zn_{0.5}mg_{0.3}Cu_{0.2}Fe_2O_4$	576	1112	1384	1632	2922	4.07
$Zn_{0.5}mg_{0.2}Cu_{0.3}Fe_2O_4$	583	1116	1382	1630	2921	4.29
$Zn_{0.5}mg_{0.1}Cu_{0.4}Fe_2O_4$	576	1117	1387	1633	2922	4.04

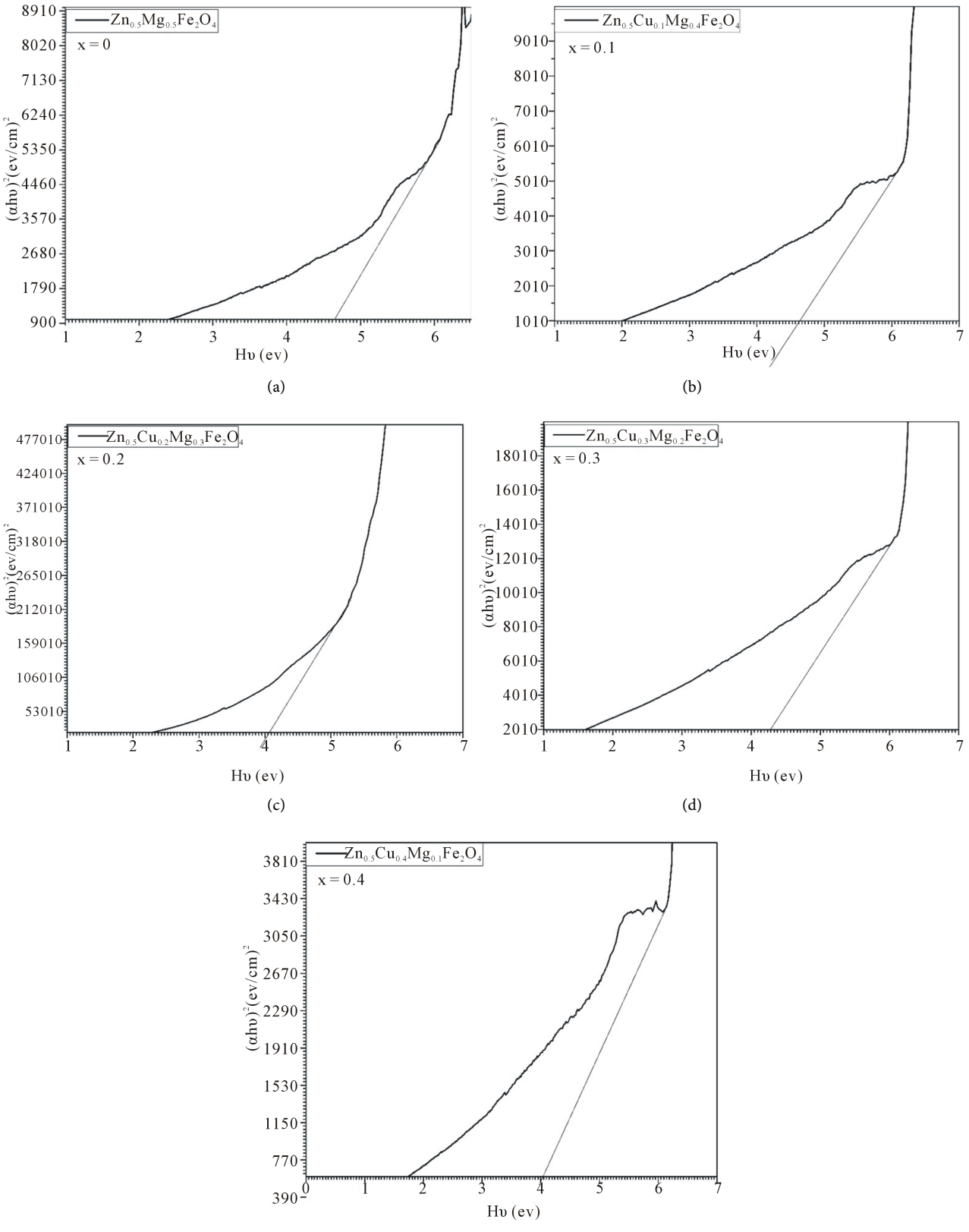

Figure 6. Plot of $(\alpha h\nu)^2$ versus hν showing the band gap of $Zn_{0.5}Cu_x\ Mg_{0.5\text{-}x}\ Fe_2O_4$ with variable Cu^{2+}doping as (a) X = 0.0; (b) X = 0.1; (c) X = 0.2; (d) X = 0.3 and (e) X = 0.4.

Respectively for the all samples; the single-phases spinel structure having two lattices tetrahedral (A) site and octahedral (B) of site [7] [22]. The band at 2921-2923 cm^{-1} is attributed to the bending vibrations of methylene (-CH_2-). The peaks at 1630 - 1633 cm^{-1} are due to the plane bending vibration of the (C-H) band bending absorption of COO^- Carboxyl group [23] [24]. The band at 1382 - 1387 cm^{-1} and is attributed to the C=O stretching vibration of the carboxyl group. In range 1112 - 1117 cm^{-1}, the band is observing and is related to the stretching vibration due to nitrate group [7] [25]. The frequency band near 576-583 cm^{-1} and 406 - 428 cm^{-1} assigned to the tetrahedral and octahedral metal oxygen (M-O) bands in the lattices of the synthesized nanocrystals [24], [26]. The FTIR frequency bands for various Cu and Mg contents are listed in **Table 2**.

3.3. UV-Visible Analysis

The diffused UV-visible absorption spectrum is recorded in order to obtain the optical band gap values of $Zn_{0.5}Cu_xMg_{0.5-x}Fe_2O_4$ as shown in **Figure 5**. The Maximum absorption displayed for sample 2 $Zn_{0.5}Cu_{0.2}Mg_{0.3}Fe_2O_4$ was occurred at 245 Cm^{-1}. However, with the doping of Cu^{2+} ion, the optical absorption properties of Nano-ferrites follow the band edge of Equation (2) (**Table 2**). In addition to that, the band gap energy was calculated for samples by Tauc plot [18] that shown in **Figures 6(a)-(d)** according to Equation (2) [17] [18].

$$\left[F\left(\left(R_\infty\right)h\nu\right)\right]^n = A\left(h\nu - E_g\right) \tag{2}$$

where α, h, ν, E_g and A are the absorption coefficient, plank constant, light frequency, band gap, and proportionality constant, respectively. The band gap values were found to be 4.67, 4.63, 4.07, 4.29 and 4.04 eV for X = 0.0, 0.1, 0.2, 0.3, and 0.4, respectively. This significant change in the band energies is due to the doping effects of Cu^{2+} ions crystal lattice [27].

4. Conclusion

Nano-ferrites samples which prepared by co-precipitation were investigated by XRD, FTIR and UV-vis. The lattice parameter was found to increase with copper concentration. Similarly, the size of crystals was found to increase from 15.97 nm to 28.33 nm. The FTIR bending vibration band of the samples confirmed the formation of spinal ferrite structure. The band gap energy calculated using Tauc plot and the absorption edge cut-off indicated that the samples possess insulator behavior.

References

[1] Mudshinge, S.R., Deore, A.B., Patil, S. and Bhalgat, C.M. (2011) Nanoparticles: Emerging Carriers for Drug Delivery. *Saudi Pharmaceutical Journal*, **19**, 129-141. https://doi.org/10.1016/j.jsps.2011.04.001

[2] Vedernikova, I. (2015) Magnetic Nanoparticles: Advantages of Using, Methods for Preparation, Characterization, Application in Pharmacy. *Review Journal of Chemi-*

stry, **5**, 256-280. https://doi.org/10.1134/S2079978015030036

[3] Kostarelos, K. (2003) Rational Design and Engineering of Delivery Systems for Therapeutics: Biomedical Exercises in Colloid and Surface Science. *Advances in Colloid and Interfacescience*, **106**, 147-168. https://doi.org/10.1016/S0001-8686(03)00109-X

[4] Mirghni, A.A., Siddig, M.A., Omer, M.I., Elbadawi, A.A. and Ahmed, A.I. (2015) Synthesis of $Zn_{0.5}Co_xMg_{0.5-x}Fe_2O_4$ Nano-Ferrites Using Co-Precipitation Method and Its Structural and Optical Properties. *American Journal of Nano Research and Applications*, **3**, 27-32.

[5] Lodhi, M.Y., Mahmood, K., Mahmood, A., Malik, H., Warsi, M.F., Shakir, I., *et al.* (2014) New $Mg_{0.5}Co_xZn_{0.5-x}Fe_2O_4$ Nano-Ferrites: Structural Elucidation and Electromagnetic Behavior Evaluation. *Current Applied Physics*, **14**, 716-720. https://doi.org/10.1016/j.cap.2014.02.021

[6] Jan, L.S., Radiman, S., Siddig, M., Muniandy, S., Hamid, M. and Jamali, H. (2004) Preparation of Nanoparticles of Polystyrene and Polyaniline by γ-Irradiation in Lyotropic Liquid Crystal. *Colloids and Surfaces A: Physicochemical and Engineering Aspects*, **251**, 43-52. https://doi.org/10.1016/j.colsurfa.2004.09.025

[7] Ahmed, A.I., Siddig, M.A., Mirghni, A.A., Omer, M.I. and Elbadawi, A.A. (2015) Structural and Optical Properties of $Mg_{1-x}Zn_xFe_2O_4$ Nano-Ferrites Synthesized Using Co-Precipitation Method. *Advances in Nanoparticles*, **4**, 45. https://doi.org/10.4236/anp.2015.42006

[8] Pardavi-Horvath, M. (2000) Microwave Applications of Soft Ferrites. *Journal of Magnetism and Magnetic Materials*, **215**, 171-183. https://doi.org/10.1016/S0304-8853(00)00106-2

[9] Spaldin, N.A. (2010) Magnetic Materials: Fundamentals and Device Applications. Cambridge University Press, Cambridge. https://doi.org/10.1017/CBO9780511781599

[10] Deraz, N. and Abd-Elkader, O.H. (2015) Structural, Morphological and Magnetic Properties of $Zn_{0.5}Mg_{0.5}Fe_2O_4$ as Anticorrosion Pigment. *International Journal of Electrochemical Science*, **10**, 7138-7146.

[11] Eltabey, M., Hassan, H.E. and Ali, I.A.E. (2014) The Electrical Properties of Mg-Cu-Zn Ferrites Irradiated by [gamma]-Rays of ^{60}Co Source. *American Journal of Applied Sciences*, **11**, 109-118. https://doi.org/10.3844/ajassp.2014.109.118

[12] Goldman, A. (2012) Handbook of Modern Ferromagnetic Materials. Springer Science & Business Media, New York.

[13] Boobalan, T., Pavithradevi, S., Suriyanarayanan, N., Raja, M.M. and Kumar, E.R. (2017) Preparation and Characterization of Polyol Assisted Ultrafine Cu-Ni-Mg-Ca Mixed Ferrite via Co-Precipitation Method. *Journal of Magnetism and Magnetic Materials*, **428**, 382-389. https://doi.org/10.1016/j.jmmm.2016.12.124

[14] Huq, M., Saha, D., Ahmed, R. and Mahmood, Z. (2013) Ni-Cu-Zn Ferrite Research: A Brief Review. *Journal of Scientific Research*, **5**, 215-234. https://doi.org/10.3329/jsr.v5i2.12434

[15] Ponpandian, N., Balaya, P. and Narayanasamy, A. (2002) Electrical Conductivity and Dielectric Behaviour of Nanocrystalline $NiFe_2O_4$ Spinel. *Journal of Physics: Condensed Matter*, **14**, 3221-3237. https://doi.org/10.1088/0953-8984/14/12/311

[16] Ahmed, M.A., Rady, K.E.-S., El-Shokrofy, K.M., Arais, A.A. and Shams, M.S. (2014) The Influence of Zn^{2+} Ions Substitution on the Microstructure and Transport Properties of Mn-Zn Nanoferrites. *Materials Sciences and Applications*, **5**, 932-942. https://doi.org/10.4236/msa.2014.513095

[17] Alsabah, Y.A., Elbadawi, A.A., Mustafa, E.M. and Siddig, M.A. (2016) The Effect of Replacement of Zn^{2+} Cation with Ni^{2+} Cation on the Structural Properties of $Ba_2Zn_{1-x}Ni_xWO_6$ Double Perovskite Oxides (X = 0, 0.25, 0.50, 0.75, 1). *Journal of Materials Science and Chemical Engineering*, **4**, 61-70. https://doi.org/10.4236/msce.2016.42007

[18] Alsabah, Y., Al Salhi, M., Elbadawi, A. and Mustafa, E. (2017) Synthesis and Study of the Effect of Ba^{2+} Cations Substitution with Sr^{2+} Cations on Structural and Optical Properties of $Ba_{2-x}Sr_xZnWO_6$ Double Perovskite Oxides (x = 0.00, 0.25, 0.50, 0.7, 1.0). *Materials*, **10**, 469. https://doi.org/10.3390/ma10050469

[19] Alsabah, Y., Elbadawi, A., Siddig, M.A. and Mohamed, I.M. (2015) Synthesis and Physical Properties of the New Double Perovskite X_2AlVO_6 (X = Ca, Sr and Ba). *International Journal of Science and Nature*, **6**, 56-62.

[20] Yue, Z., Zhou, J., Li, L. and Wang, X.G. (2001) Effect of Copper on the Electromagnetic Properties of Mg-Zn-Cu Ferrites Prepared by Sol-Gel Auto-Combustion Method. *Materials Science and Engineering: B*, **86**, 64-69. https://doi.org/10.1016/S0921-5107(01)00660-2

[21] Rezlescu, N., Rezlescu, E., Popa, P.D., Craus, M.L. and Rezlescu, L. (1998) Copper Ions Influence on the Physical Properties of a Magnesium-Zinc Ferrite. *Journal of Magnetism and Magnetic Materials*, **182**, 199-206. https://doi.org/10.1016/S0304-8853(97)00495-2

[22] Singhal, S., Bhukal, S., Singh, J., Chandra, K. and Bansal, S. (2011) Optical, X-Ray Diffraction, and Magnetic Properties of the Cobalt-Substituted Nickel Chromium Ferrites ($CrCo_xNi_{1-x}FeO_4$, x = 0, 0.2, 0.4, 0.6, 0.8, 1.0) Synthesized Using Sol-Gel Autocombustion Method. *Journal of Nanotechnology*, **2011**, Article ID: 930243.

[23] Aad, G., Abbott, B., Abdallah, J., Abdelalim, A., Abdesselam, A., Abdinov, O., *et al.* (2011) Measurement of Inclusive Jet and Dijet cross Sections in Proton-Proton Collisions at 7 TeV Centre-of-Mass Energy with the ATLAS Detector. *The European Physical Journal C*, **71**, 1512. https://doi.org/10.1140/epjc/s10052-010-1512-2

[24] Singh, C., Bansal, S. and Singhal, S. (2014) Synthesis of $Zn_{1-x}Co_xFe_2O_4$/MWCNTs Nanocomposites Using Reverse Micelle Method: Investigation of Their Structural, Magnetic, Electrical, Optical and Photocatalytic Properties. *Physica B: Condensed Matter*, **444**, 70-76. https://doi.org/10.1016/j.physb.2014.03.033

[25] Hankare, P., Patil, R., Jadhav, A., Pandav, R., Garadkar, K., Sasikala, R., *et al.* (2011) Synthesis and Characterization of Nanocrystalline Ti-Substituted Zn Ferrite. *Journal of Alloys and Compounds*, **509**, 2160-2163. https://doi.org/10.1016/j.jallcom.2010.10.173

[26] Waldron, R. (1955) Infrared Spectra of Ferrites. *Physical Review*, **99**, 1727-1735. https://doi.org/10.1103/PhysRev.99.1727

[27] Chavan, S., Babrekar, M., More, S. and Jadhav, K. (2010) Structural and Optical Properties of Nanocrystalline Ni-Zn Ferrite Thin Films. *Journal of Alloys and Compounds*, **507**, 21-25. https://doi.org/10.1016/j.jallcom.2010.07.171